HHS Public Access

Author manuscript

Cell Rep. Author manuscript; available in PMC 2016 January 09.

Published in final edited form as:

Cell Rep. 2016 January 5; 14(1): 129–139. doi:10.1016/j.celrep.2015.12.019.

Epilepsy-related Slack channel mutants lead to channel over-activity by two different mechanisms

Qiong-Yao Tang[1,2], **Fei-Fei Zhang**[1,2], **Jie Xu**[1,2], **Ran Wang**[3], **Jian Chen**[3], **Diomedes E Logothetis**[4], and **Zhe Zhang**[1,2]

[1]Jiangsu Province Key Laboratory of Anesthesiology, Xuzhou Medical College, Xuzhou, Jiangsu Province, 221004, CHINA

[2]Jiangsu Province Key Laboratory of Anesthesia and Analgesia Application Technology, Xuzhou Medical College, Xuzhou, Jiangsu Province, 221004, CHINA

[3]School of Anesthesiology, Xuzhou Medical College, Xuzhou, Jiangsu Province, 221004, CHINA

[4]Department of Physiology and Biophysics, Virginia Commonwealth University, Medical College of Virginia Campus, Richmond, VA, 23298, USA

Summary

Twelve sodium-activated potassium channel (KCNT1, Slack) genetic mutants have been identified from severe early-onset epilepsy patients. The changes in biophysical properties of these mutants and the underlying mechanisms causing disease remain elusive. Here we report that seven of the twelve mutations increase, while one mutation decreases the channel's sodium sensitivity. Two of the mutants exhibit channel over-activity only when the intracellular Na^+ ($[Na^+]_i$) concentration is approximately 80 mM. In contrast, single channel data reveal that all twelve mutants increase the maximal open probability (P_o). We conclude that these mutant channels lead to channel over-activity predominantly by increasing the ability of sodium binding to activate the channel, which is indicated by its maximal P_o. The sodium sensitivity of these epilepsy causing mutants probably determines the $[Na^+]_i$ concentration at which these mutants exert their pathological effects.

Graphical Abstract

Corresponding to zhangzhe70@xzmc.edu.cn.

Author contributions

QY.T and Z.Z. initiated the study. QY.T. and Z.Z. made key experimental observations. FF. Z, R.W and J.C performed molecular cloning and mutant construction. J.X performed molecular modeling, which provided images in Figure 1 and Figure 3. QY.T, Z.Z performed experiments in Figures 2–6. Z.Z, FF. Zhang and J.X performed data analysis that had been used in Figures 2–7. QY.T, and Z.Z wrote the manuscript, which was revised by D.E.L.

Supplemental information

Supplemental Information for this article includes six supplemental figures.

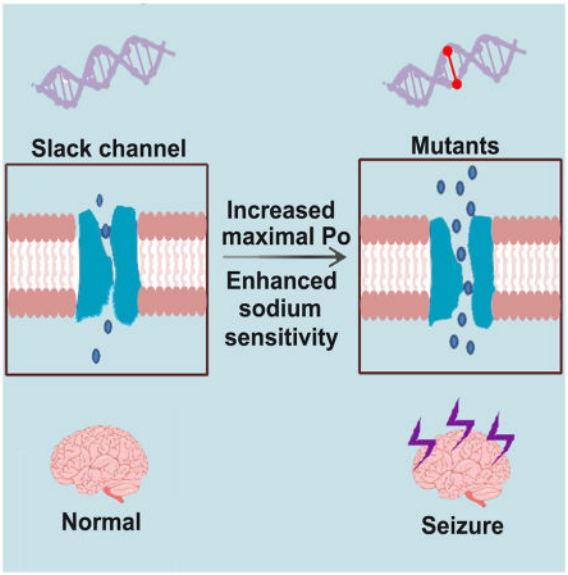

Introduction

Sodium activated potassium channels were first identified from guinea pig cardiac cells (Kameyama et al., 1984). Subsequent studies demonstrated that these channels are encoded by the Slack gene, which belongs to the Slo channel family that includes Slo1, Slo2 and Slo3 (Salkoff et al., 2006; Yuan et al., 2003). Slack channels are widely expressed in the brain, heart and dorsal root ganglia (DRG) (Bhattacharjee et al., 2002; Bhattacharjee et al., 2005; Joiner et al., 1998; Yuan et al., 2003). Their functions include modulating neuron rhythmic firing (Brown et al., 2008; Yang et al., 2007), regulating pain sensation (Gao et al., 2008; Huang et al., 2013; Tamsett et al., 2009), and being involved in intellectual disability (Brown et al., 2010; Kim and Kaczmarek, 2014; Zhang et al., 2012). Recently, twelve Slack channel mutants were identified from patients who presented with early-onset epilepsy disease (Barcia et al., 2012; Heron et al., 2012; Ishii et al., 2013; Vanderver et al., 2014). Most of them were identified from patients with the malignant migrating partial seizure of infancy (MMPSI) and the autosomal dominant nocturnal frontal lobe epilepsy (ADNFL) (Figure 1A). At present, whether there are functional changes in the properties of Slack channels as a consequence of these mutations remains elusive. Here we therefore have examined whether there are any changes in gating or changes in Na^+ sensitivity. Sodium binding has been shown to be the most important gating regulator of Slack channels, although PIP_2, Cl^- and phosphorylation have also been reported to be involved in the regulation of channel gating (Barcia et al., 2012; de los Angeles Tejada et al., 2012; Yuan et al., 2003). Recently, we reported identification of a sodium sensitive site that is located in the RCK2 domain of Slack channels that contains a similar amino acid sequence motif as the GIRK2 and GIRK4 channel sodium binding sites (Zhang et al., 2010). Although the Slack channels use a similar sequence motif as the GIRK channel sodium binding site, the sodium sensitivity K_d value of Slack channel is markedly higher than the K_d value of the GIRK2 channel. In addition, whether or not other domains are also involved in sodium sensing remains unknown. Thus, systematically characterizing sodium sensitivity of these mutants

may provide insights into loci on the Slack channel that are important in regulating channel function. The Slack channel forms a tetramer in the membrane with four identical subunits encoded by the Slack gene. Each subunit is composed of 6 membrane- spanning segments with both the N terminus and long C terminus positioned in the cytosol. The tetrameric Slack channel shares with other Slo family members a large cytosolic domain termed a gating ring that is thought to contain ligand binding sites that regulate channel gating. Although detailed structural information about this channel is still not available, recently solved C terminal domain structures of the Slo1 channel have provided good templates to build homology models of this channel. In fact, a low resolution crystal structure of the Slack C-terminal domain shows high similarity with the 3D structure of the Slo1 C terminal domain (Wu et al., 2010; Yuan et al., 2010). Thus, the homology models could provide useful information regarding the structural basis of sodium sensitivity changes induced by some of the epilepsy-causing mutants.

In addition to sodium sensitivity, the gating behavior of Slack channels could also be altered by the ability of sodium binding to activate the channel, as determined by the maximal channel open probability (P_{max}) that requires saturating sodium binding, analogous to changes in potency (Na sensitivity) versus efficacy (P_{max}) of $[Na^+]_i$ on open probability. This P_{max} change may also be the basis for the association of these mutations with neurological disorders. Consequently, we further measured the single channel level P_o over a complete range of $[Na^+]_i$. These data can distinguish the different roles of these mutants on influencing two distinct steps that activate Slack channels: a recognition event in which sodium binds to the channel and a conformational change that opens the channel. We also further tested different combinations of these mutants to investigate whether the regulatory effects of each mutant exert mutual influences.

Taken together, our data involving systematic measurements of the sodium sensitivity by recording macroscopic current and unitary opening probability of these mutated channels over a complete range of $[Na]_i$, revealed that a total of seven mutations increase the sodium sensitivity of this channel, while one mutation decreases its sodium sensitivity. More importantly, single-channel analysis indicates all these mutants resulted in a gain-of-function phenotype with increased maximal P_o. However, two mutants exhibit their over-activity only at high concentrations of intracellular sodium due to changes in sodium sensitivity. Thus, our results not only suggest that epilepsy related mutants lead to channel over-activity based on two distinct mechanisms, but also indicate the sodium sensitivity of these mutants is likely to determine the condition on which these mutants are associated with epilepsy.

Results

Certain mutants lead to channel over-activity by enhancing the sodium sensitivity of Slack channels

We performed experiments on the rat Slack channel, which is highly homologous to the human Slack channel. Epilepsy-related mutant amino acid sequence numbers are labeled and shown in schematic representation (Figure 1A). The epilepsy related mutants are distributed widely, including positions in the pore domain, the RCK1 and RCK2 domains (Figure1A and 1B). Their positions are also indicated on a homology model constructed

using a template that superimposed the Kv1.2/2.1 pore domain on the Slo1 C-terminus (Figure 1B). The epilepsy-related mutants are located on segments that, in general, are highly conserved among members of the mammalian Slack channel subfamily (Figure 1C). We first measured the sodium sensitivity of Slack channel mutants using the inside-out patch configuration. Macroscopic currents were recorded over a wide range of intracellular sodium concentrations ($[Na^+]_i$) from 0 mM to 500 mM by a ramp protocol from −100 mV to +100 mV (Figure 2A–C). The current level at −90 mV in different $[Na^+]_i$ was measured to assess the sensitivity of wild-type and mutant Slack channels to Na^+ as previously described (Zhang et al., 2010). The current levels measured in different Na^+ concentrations were normalized to the current level at 250mM Na^+ and were fitted with the Hill equation to obtain K_d values of the channel's sodium sensitivity. In order to avoid run-down of some patches confounding the results, we selected patches without significant run-down in the following way: currents were measured from 500 mM to 0 mM $[Na^+]_i$ within 5 minutes, then measured again at the end of the experiment at 500 mM (or 250 mM) $[Na^+]_i$. Only patches which maintained a similar current level (<3% run down) in response to 500 mM (or 250 mM) $[Na^+]_i$ were used for analysis (Figure S1). The overall results show that Y775H and six other mutations (V252F, G269S, R409Q, R455H, R907C and A913T) significantly enhanced sodium sensitivity of Slack channels (labeled with * in Figure 2F), while one mutation R379Q significantly decreased sodium sensitivity of Slack channels (Figure 2E, labeled with * in Figure 2F). Other mutations (e.g. A945T) did not significantly alter the sodium sensitivity of Slack channels (Figure 2D and 2F). Sodium sensitivity K_d of Y775H was 35mM, which is almost 2 fold lower than the K_d value of the wild-type Slack (K_d = 68 mM) (Figure 2E). Interestingly, this sodium sensitivity value is close to the K_d values of the sodium-activated GIRK channels (GIRK2 and GIRK4). To further investigate the mechanism by which Y775H enhances the sodium sensitivity of Slack channels, we tested additional Y775 mutants. Typical traces and normalized currents of Y775D, Y775F, and Y775E fitted with the Hill equation are also shown (Figure 3A–B). We found that the Y775D mutation had an even stronger effect than the Y775H mutation in enhancing the sodium sensitivity of Slack channels with a K_d value of 18 mM (Figure 3C, * indicates mean values significantly different from the wild-type Slack channel). As we recently reported, Slack channels use a similar sodium binding motif as GIRK channels, and thus we speculated that the Y775H mutation may mimic the role of the critical amino acid GIRK2 channel residue H69 in the sodium binding site (Whorton and MacKinnon, 2011), in which a negatively charged residue, Asp228, coordinates Na^+ binding by the carboxylate residue and two flanking histidine amino acids, H233 and H69 (Whorton and MacKinnon, 2011; Rosenhouse et al., 2008). To test this idea, we set up homology models of the wild-type Slack channel, Y775H and Y775D mutants by using the Slo1 C-terminal crystal structure as a template. Then, we compared the local structure of the sodium binding site in these models. The local structure of the sodium binding site in the model of the wild-type Slack channel shows that the Y775 does not seem to be involved in sodium binding because the phenol ring of Y775 is not parallel to the nitrogen ring of H823 and thus cannot form a sandwich-like structure with H823 to flank a sodium ion. (Figure 3D nitrogen atoms on the ring of H823 residue are shown in blue, other bonds are shown in cyan; sodium ion is indicated by upper yellow sphere). But on the model of the Y775H mutant, the nitrogen ring of H775 appears to be parallel to the nitrogen ring of H823. The negatively charged residue

D818 can coordinate Na^+ along with the two flanking histidine residues H823 and H775 to form a local structure similar to the local structure of the GIRK2 sodium binding site (Figure 3E nitrogen atoms on ring are shown in orange. The sodium ion is indicated by the lower yellow sphere). In addition, the model of the Y775D mutant indicates that the D775 residue can cooperate with the D818 residue to form stronger electrostatic interaction that co-ordinates Na^+ to enhancing the sodium binding affinity (Figure 3F). In other words, the Y775D may stabilize the sodium binding conformation of the Slack channel. These data suggest that Y775H is involved in sodium sensing.

On the RCK1 domain of Slack channels, three mutants (R379Q, R409Q and R455H) were identified in epilepsy patients. Their normalized current levels in different concentrations $[Na^+]_i$ were fitted by the Hill equation (Figure 4A–C). The K_d value of R379Q mutant was 79 mM while the K_d values of the R409Q, R455H mutants were 45 mM and 55 mM, respectively (Figure 2F and Figure 4A–C). Thus, the R379Q mutation decreased the channel's sodium sensitivity, while the R409Q and R455H mutations increased it. To test whether the effect of these mutations influence each other, we measured the sodium sensitivity of double and triple mutants. Typical traces and Hill equation fits are shown (Figure 4D–E). The double mutant R409Q/R455H yielded an enhanced sodium sensitivity with a K_d value of 18 mM (Figure 4F, * indicates mean values significantly different from the wild type channel). In contrast, the R379Q/R409Q/R455H triple mutant and the R379Q/Y775H double mutant partially offset the sodium sensitivity-enhancing effect of the R409Q/R455H and Y775H mutants (Figure 4F), as the K_d value shifted back to 44 mM and 49 mM, respectively. These results indicate that the conformational changes induced by these mutations altered the sodium sensitivity of Slack channels independently.

Single channel recording revealed that all epilepsy-associated mutations increased the maximal open probability Figure of Slack channels

To further test the sodium sensitivity change of these mutants, we systematically measured the channel open probability (Po) over a complete range of $[Na^+]_i$ using single-channel recordings. Typical traces of Y775H, R379Q and R455H in 50 mM, 100 mM and 200 mM $[Na^+]_i$ are shown (Figure 5A–C). Hill equation fits of the P_o of all these mutants in different $[Na^+]_i$ concentrations further confirmed the sodium sensitivity change of these mutant channels (Figure 5D–F). The best Hill equation fits of the R379Q and R409Q show higher co-factor numbers than that of the wild type and other mutants, reflecting greater cooperativity among different Slack channel subunits (Figure 5D–E). Overall, consistent with macroscopic current results, the seven mutants showed significantly decreased K_d values of sodium sensitivity while the R379Q mutant exhibited an enhanced K_d value of sodium sensitivity (Figure 5F). More importantly, single channel open probability analysis clearly indicates that the R455H and Y775H mutations enhance not only the sodium sensitivity but also the P_{max} of the Slack channel (Figure 5D–E). In contrast the R379Q mutant decreased Na^+ sensitivity but increased the channel's P_{max}. Further analysis of the P_o over a complete range of $[Na^+]_i$ showed a significant P_{max} increase in all twelve mutant channels. The I739M mutant did not yield a significant change in Na^+ sensitivity (Figure 2F) but did increase P_{max}. Typical unitary conductance traces of wild-type Slack channel and the I739M mutant are shown in FigureS2.A. Amplitude histograms fitted by Gaussian functions

reveal that this mutant demonstrates higher channel activity than the wild type Slack channel activity in any given sodium concentration, even though the sodium sensitivity of this mutant was not enhanced (Figure S2. B–G). The summarized data indicate the P_{max} of all epilepsy related mutants were increased from 53% to 70%–90% by 500 mM Na^+ (Table S1 and Table S2). This result suggests that increased P_{max} was the predominant reason that these mutants lead to channel over-activity. No significant unitary conductance change and temperature sensitivity was observed on any of these mutant channels (Figure S3 and Figure S4).

The R409Q/R455H double mutant shows significant channel opening without intracellular sodium

In order to test whether the P_{max} of the double mutant R409Q/R455H could be further increased, we proceeded to record and analyze single-channel currents of this mutant. Typical traces of single channel recording and Gaussian equation fits are shown (Figure 6A–C). Our data indicate that the P_{max} of R409Q/R455H could not be further increased, but some channel openings of this double mutant could be observed even in 0 mM $[Na^+]_i$ (Figure 6A and B, Table S1). Consistent with the macroscopic currents, the single-channel data analysis shows that this mutation also enhanced Na^+ sensitivity of Slack channels. The P_o of this mutant channel is much higher than the wild-type Slack channel P_o in any given sodium concentration (Figure 6D). The small P_o in 0 $[Na^+]_i$ suggests that mutual interaction of these two mutant residues triggers a critical conformational change that can stabilize the transient state of activation independently of sodium binding.

Sodium sensitivity of the mutant channels determines the condition on which mutant channels demonstrate over-activity

The P_o data over a complete range of $[Na^+]_i$ of these mutants were summarized and shown in Table S1 and Table S2. All mutants led to channel over-activity at saturating sodium concentrations. However, at a concentration of 25 mM $[Na^+]_i$, some mutants still showed lower channel activity than the wild-type Slack channel activity (Table S1 and Table S2). For the R379Q and R409Q mutants, the open probabilities were less than the wild-type P_o of Slack channels even at 50 mM $[Na^+]_i$ (Figure 7A). Not until the $[Na^+]_i$ was close to 100 mM, were the R379Q and R409Q P_o values higher than the P_o of wild-type Slack channels (Figure 7B and 7C). These results suggest that if the channel over-activity is the reason of these mutants leading to epilepsy, then these two mutants would not exert their pathological influence when the intracellular sodium concentration is lower than 80 mM.

Based on all the data presented in this article, we conclude that epilepsy-related Slack channel mutants lead to channel over-activity by increasing P_{max} with or without enhancing sodium sensitivity. Yet, the sodium sensitivity of these mutant channels determines at which Na^+ concentration these mutants lead to channel over-activity. On the RCK1 domain, the R379Q, R409Q and R455H mutants regulate sodium sensitivity independently, as suggested by the additive regulatory effect of the double or triple mutants. The R409Q/R455H double mutant shifts the intrinsic closing and opening rates through stabilization of the activation state without agonist binding. On the RCK2 domain, the Y775H mutation may be part of the sodium site, but we cannot completely exclude the possibility that it just changes the

coupling between sodium binding and channel opening due to the complexity of conformational transitions (Colquhoun, 1998).

Discussion

This study characterizes the functional properties of all reported Slack channel mutants that relate to epilepsy. We found that these mutations lead to Slack channel over-activity by two different mechanisms: increasing P_{max} or increasing sodium sensitivity. The former is the dominant mechanism because all mutants show increased P_{max} at saturating sodium concentrations. The latter can further increase channel activity on some of the mutants at any given sodium concentration. These results have offered insight into possible mechanisms by which these mutants are associated with epilepsy. However, our data also indicate that two mutants would only lead to channel over-activity if the intracellular sodium concentration could rise to 80 mM (Figure 7). Furthermore, if the channel over-activity is the reason that these mutants result in epilepsy, then the two mutants cannot exert their pathological role unless the intracellular sodium concentration reaches that level. However, in neurons at the resting membrane potential, the global intracellular Na^+ concentration is between 4–15 mM (Bhattacharjee and Kaczmarek, 2005; Rose and Karus, 2013). Even under hypoxic conditions, Na^+ levels only reach 27 mM (Muller and Somjen, 2000). Thus, it seems unlikely that the global intracellular Na^+ concentration would ever reach 80 mM. Yet, previous studies have found that persistent Na^+ currents have been observed on the dendrites of many kinds of neurons (Callaway and Ross, 1997; Mittmann et al., 1997). Thus, the local sodium concentration may reach a very high level (Kleinhans et al., 2014). Furthermore, recent studies have identified novel sodium channels that are responsible for persistent sodium currents and link the persistent sodium current with Slack channels (Hage and Salkoff, 2012; Lu et al., 2007). In addition, Slack channels are highly expressed on the dendrites of neurons (Bhattacharjee and Kaczmarek, 2005; Bhattacharjee et al., 2005; Egan et al., 1992). Therefore, dendrite synaptic connectivity and neuronal excitability will require future studies to accurately discern physiological function of Slack channels and the pathological effect of Slack channel mutants. Moreover, intracellular sodium levels have been reported as an important factor in controlling seizures (Fekete et al., 2009). Whether patients carrying mutant channels that are over-activated in low intracellular sodium concentration show more serious symptoms, have different prognosis or need additional treatment strategies will need to await further clinical investigation.

But if over-activation of the Slack channel is associated with epilepsy, an intriguing question that needs to be answered is how over-activation of the Slack channel influences neuronal excitability. Epileptic seizures result from excessive and abnormal cortical nerve cell activity in the brain (Fisher et al., 2005). Membrane depolarization and repolarization are the fundamental phases of the action potential, which are critical for neuronal activation within the nervous system, mediated by neurotransmitters such as glutamate or GABA acting on their respective receptor channels. Over-activation of potassium channels usually leads to hyperpolarization and decreases excitability of the neuron in which they are expressed. From published work, both loss- and gain-of-function potassium channel mutants had been linked to epilepsy. Among them, loss-of-function of Kv1.1, Kv1.2, Kv4.2 and Kv7.1, Kv7.2 potassium channels are associated with epilepsy (Brew et al., 2007; D'Adamo et al., 2013;

Smart et al., 1998; Wang et al., 2015; Zeng et al., 2015). On the other hand, gain-of-function of the BK and Slack channel mutants are also linked with Epilepsy (Barcia et al., 2012; Du et al., 2005; Yang et al., 2010). One plausible explanation that can reconcile these contradictory findings is that these potassium channels may be expressed in different types of neurons, namely excitatory versus inhibitory. Furthermore, when the potassium channels are expressed in excitatory neurons, the loss-of-function of potassium channel will increase the activation of excitatory neurons by facilitating depolarization, such as with Kv channels. In contrast, over-activation of Slack channel or BK channels may dampen the excitability of inhibitory neurons and lead to decreased inhibitory neurotransmitter release, such as GABA. Thus, it may facilitate synchronization of activation of excitatory neurons and decrease the threshold of epilepsy. Indeed, Slack channels are expressed in frontal lobes, in which GABAergic inhibitory neurons are rich (Bhattacharjee et al., 2002; Joshi et al., 2012; Soumier and Sibille, 2014). Although this compelling hypothesis will need further investigation, epilepsy associated loss-of-function mutants of the sodium channel 1.1 in inhibitory neurons have been reported (Lossin et al., 2003; Yu et al., 2006). In order to test if these mutants decreased cell surface expression level of channels as to offset the channel over-activation effect, we measured patch currents levels of Slack channel and mutants under similar conditions (see also experimental procedures). The normalized cell surface expression levels of Slack channel and its mutants did not show statistical differences (Figure S5). We also examined the temperature sensitivity of Slack channel and its mutants by single channel recording. We did not find any mutant is sensitive to temperature (Figure S4).

It has been shown previously that a sodium binding motif identified from Kir channels, DXRXXH, is localized on the RCK2 domain of Slack channels (Zhang et al., 2010). A recently solved crystal structure of the GIRK2 channel has provided greater detail on the local structure of this sodium co-ordination site. Another amino acid residue, H69, that is not part of this motif is also involved in forming the sodium binding site (Whorton and MacKinnon, 2011). In the current study, by combining electrophysiology data (Figure 3A–C) and homology modeling, we provide compelling evidence that the H775 residue plays a critical role in the sodium co-ordination site of the Slack channel, as H69 plays in the Na^+ co-ordination site of the GIRK2 channel. This result suggests that the conserved structure element of the Na^+ sensor in distinct potassium channels is fine-tuned by specific elements in each channel. However, fully addressing detailed local structure of sodium binding site still needs to wait high resolution crystal structure of Slack channel with sodium binding is solved.

These results also show that mutants on the RCK1 domain (R379Q, R409Q and R455) and pore domain (V252F and G269S) significantly alter the sodium sensitivity of Slack channels. But whether these mutants are allosterically involved in sodium sensitivity or just decrease the energetic barrier of coupling sodium binding with channel activation will require future work. In contrast with the gating properties of the Slo1 and Slo3 channel, Slack channel activation is not voltage dependent. Thus, the Slack channel is almost a purely intracellular ligand-activated channel. Consequently, the gating model of Slack channels is different from that of BK channels. Yet, the intrinsic conformation transition independent of ligand binding may still exist in the Slack channel because the double mutant R409Q/R455H

enhances sodium independent channel opening, reflecting a unique conformational change enhancing the intrinsic C-O transition equilibrium. Thus, we tried to use the MWC model to describe the gating behavior of the Slack channel and its mutants. The individual subunit C-O equilibrium is represented by factor L in the model of Figure S6. A. The Slack channel also undergoes a conformational transition with 0–4 sodium ions binding. This equilibrium is represented by K. The interaction between sodium binding and channel opening is represented by factor D, the ratio of K/Ko between closed and open states, which reflects the ability of sodium binding to activate Slack channel as indicated by P_{max} (Figure S6. A). The four subunits conformation change of this model can be described by the scheme shown in Figure S6. B. A detailed fit with this model for each mutant will require more work and further adjustment of this model, which is beyond the scope of the present paper. Our single channel analysis clearly shows that all these mutations enhance the ability of sodium binding to activate Slack channels by increasing factor D.

The structural basis of the conformational changes triggered by these mutations is intriguing. The model that a gating ring composed of RCK1 and RCK2 domains expands and pulls on the linkers of the channel gates to open the channel upon Ca^{2+} binding had been proposed for Slo1 channels (Jiang et al., 2002a, b; Niu et al., 2004). Considering the similar C-terminal structure of Slo family members, a similar mechanism may also be utilized by Slack channels. Our findings provide important loci on the RCK domains and pore domain that regulate coupling of ion-sensing to channel gating. Revealing the structural basis of this coupling in terms of the molecular details that are involved still needs to await elucidation of the structure of the Slack channel.

A very recent study of these mutants was published by Kim and colleagues attributing the channel over-activity to cooperativity of clustered mutant channels (Kim et al., 2014). However, in our study the increase in the maximal Po and the enhancement of the sodium sensitivity could be observed in single-channel recordings in excised patches. The simplest explanation for the different conclusions of two groups is that the single-channel data used in the published paper were obtained from cell-attached patches containing multiple channels. Thus, the P_o measured in this configuration was not obtained from a given intracellular sodium concentration and could not be used to compare each mutant. We successfully used excised inside-out patches taking into account activity rundown (Figure S1) and strictly controlled sodium concentration. Therefore, we believe our conclusions are sound.

Experimental Procedures

Mutagenesis and expression

The Slack-B construct (Gene ID: 60444) was a gift from Dr. Kaczmarek. Slack mutations were generated by Pfu-based mutagenesis using the Quick Change TM kit and verified by sequencing, as published previously (Zhang et al., 2010; Zhang et al., 2013). RNA was transcribed in vitro with T3 polymerase (Ambion, TX) and cRNAs of each channel were prepared at a concentration of ~0.5g/μl. Each *Xenopus* oocyte was injected with 2~20 ng of cRNA depending on the expression level of the given channel protein. Single channel

currents were normally recorded within 5-days, and macroscopic currents within ~10 days (Tang et al., 2014; Tang et al., 2010).

Electrophysiology

Macroscopic and single channel currents were recorded from standard excised inside-out patches with an A-M 2400 patch clamp amplifier (A-M systems, Inc) or HEKA EPC10 patch clamp amplifier. Data were filtered at 10 KHz. All currents were recorded within 5 min after patch excision to minimize significant rundown, and only patches that did not show rundown were included in the analysis. Patch-clamp recording pipettes were made from borosilicate capillary tubes (PG10150-4; World Precision Instruments) and had resistances of 1–2 MΩ. The standard pipette/extracellular solution was ND96K–EGTA solution [in mM]: 90 KMES, 20 HEPES-K, 2 $MgCl_2$ and 50 EGTA-K-02/06M (200 mM EGTA and 600 mM KOH), pH7.4. Bath/intracellular solutions contained the following (in mM): 90 mM KMES, 20 HEPES-K, 50 EGTA-K-02/06M, and 0–500 NaGlu. Gigaohm seals were formed in ND96K–EGTA solution with 0 Na^+. Experiments were performed at room temperature (22–25°C) except as specified in the data of Figure S4. The dish temperature at 34°C was maintained by a Warner warm platform. Salts of the compounds mentioned were purchased from Sigma.

For comparing the cell surface expression levels of Slack channel and mutants, Slack channel and mutants RNA were diluted to 600ng/ul, 42 nl RNA were injected into each oocyte. The pipette resistances were controlled between 1–2 Mohms. The currents of inside-out patch were recorded from 4–5 days after injection. Currents were measured at −100 mV with 250 $[Na^+]_i$. Mutant currents of each patch (I_m) were firstly divided by the ratio of averaged Po of each mutant (Po_m) to averaged Po of wild type (Po_w) at 250 mM $[Na^+]_i$ based on data summarized in Table S1 and Table S2, then it was divided by the averaged wild-type patch current level (I_w) to get a normalized expression level of mutants(NE_m). $NE_m=I_m/(Po_m/Po_w)/I_w$.

Homology Modeling

The Slack homology model used in Figure 1 was generated based on the crystal structures of Kv1.2/2.1 (PDB code: 2R9R) and hSlo1 structure (PDB code: 3NAF). In order to develop the Slack channel homology model, we first built a hybrid template of 2R9R-3NAF, which is composed of membrane-spanning structure (S1–S6) of the Kv1.2/Kv2.1 and of the hSlo1 cytoplasmic structure as described in Tang et al (Tang et al., 2014), the membrane-spanning structure (the Kv1.2/Kv2.1 S1–S6) was docked onto the hSlo1 cytoplasmic structure based on the orientation of the four S6-RCK1 linkers of hSlo1 structure (3NAF), the Slack mutants were then generated by sequence alignment using the Clustal W server with manual adjustments in non-homologous regions.

The C-terminal homology models used in Figure 3 were then generated based on hSlo1 cytoplasmic domain (3NAF) crystal. We use the Swiss model website (http://swissmodel.expasy.org/) to build up this model by following the website instruction. The homology models of Y775H and Y775D mutants were generated by using a fully automated

Swiss model algorithm, the energy minimization was performed by using the GROMOS96 force field.

Single channel Analysis

Single-channel conductance values were measured from −120mV to −40 mV. I–V data were fitted to a linear line. Amplitude histograms were measured in inside-out patches with 1 to 4 channels. Histograms were fitted with a Gaussian function using the software ANA.EXE. The open probability P_o (%) of the channels was determined as described previously (Zhang et al., 2010). The open probability (*P*o) of the channels was calculated using the area under each peak (*aj*) at each current level (*j*) in the histogram along with the number of channels (*N*) as follows:

$$\mathrm{Po}=\frac{\sum_{j=0}^{N}(j*aj)}{n\times\sum_{j=0}^{N}\mathrm{aj}} \quad (1)$$

The channel numbers in each patch was defined as the largest opening channel numbers that can be observed at 500 mM $[Na^+]_i$. The Hill equation was used to fit the P_o in different concentrations of $[Na^+]_i$ to determine Hill coefficient factor (n) and the K_d that is required to open half of the maximum P_o of the channels.

Data Analysis

Data acquisition and analysis were carried out using pClamp9 (Molecular Devices), ANA.EXE and Origin7.5 software. The macroscopic current recorded in different concentration of $[Na^+]_i$ were normalized to the current at 250 mM Na^+. The K_d values were calculated by fitting with Hill equation. Data in all figures are expressed as mean ± SEM. Statistical significance was evaluated by One Way Anova and $p\leq0.05$ was considered as significant.

Supplementary Material

Refer to Web version on PubMed Central for supplementary material.

Acknowledgments

The Slack clone was kindly provided by Dr. Kaczmarek (Yale University School of Medicine, New Haven, CT). This work was supported by The Important Project of Natural Science in Colleges and Universities in Jiangsu Province to Z.Z (14KJA320002), Jiangsu specially-appoint professorship to Z.Z and QY.T, NSFC grant to Z.Z (81471314), NSFC grant to QY.T (81450064), NIH grant to D.E.L (R01HL59949). We also appreciated the grant support from the Priority Academic Program Development of Jiangsu Higher Education Institutions and grant from Jiangsu Provincial Special Program of Medical Science (BL2014029), Training Programs of Innovation and Entrepreneurship for undergraduates of Jiangsu province in 2014 (201410313017Z), Training Programs of Innovation and Entrepreneurship for undergraduates of china in 2014 (201410313017) to W.R. We thank Chris Lingle for helpful suggestions and comments.

References

Barcia G, Fleming MR, Deligniere A, Gazula VR, Brown MR, Langouet M, Chen H, Kronengold J, Abhyankar A, Cilio R, et al. De novo gain-of-function KCNT1 channel mutations cause malignant migrating partial seizures of infancy. Nat Genet. 2012; 44:1255–1259. [PubMed: 23086397]

Bhattacharjee A, Gan L, Kaczmarek LK. Localization of the Slack potassium channel in the rat central nervous system. J Comp Neurol. 2002; 454:241–254. [PubMed: 12442315]

Bhattacharjee A, Kaczmarek LK. For K+ channels, Na+ is the new Ca2+ Trends Neurosci. 2005; 28:422–428. [PubMed: 15979166]

Bhattacharjee A, von Hehn CA, Mei X, Kaczmarek LK. Localization of the Na+-activated K+ channel Slick in the rat central nervous system. J Comp Neurol. 2005; 484:80–92. [PubMed: 15717307]

Brew HM, Gittelman JX, Silverstein RS, Hanks TD, Demas VP, Robinson LC, Robbins CA, McKee-Johnson J, Chiu SY, Messing A, Tempel BL. Seizures and reduced life span in mice lacking the potassium channel subunit Kv1.2, but hypoexcitability and enlarged Kv1 currents in auditory neurons. J Neurophysiol. 2007; 98:1501–1525. [PubMed: 17634333]

Brown MR, Kronengold J, Gazula VR, Chen Y, Strumbos JG, Sigworth FJ, Navaratnam D, Kaczmarek LK. Fragile X mental retardation protein controls gating of the sodium-activated potassium channel Slack. Nat Neurosci. 2010; 13:819–821. [PubMed: 20512134]

Brown MR, Kronengold J, Gazula VR, Spilianakis CG, Flavell RA, von Hehn CA, Bhattacharjee A, Kaczmarek LK. Amino-termini isoforms of the Slack K+ channel, regulated by alternative promoters, differentially modulate rhythmic firing and adaptation. J Physiol. 2008; 586:5161–5179. [PubMed: 18787033]

Callaway JC, Ross WN. Spatial distribution of synaptically activated sodium concentration changes in cerebellar Purkinje neurons. J Neurophysiol. 1997; 77:145–152. [PubMed: 9120555]

Colquhoun D. Binding, gating, affinity and efficacy: the interpretation of structure-activity relationships for agonists and of the effects of mutating receptors. Br J Pharmacol. 1998; 125:924–947. [PubMed: 9846630]

D'Adamo MC, Catacuzzeno L, Di Giovanni G, Franciolini F, Pessia M. K(+) channelepsy: progress in the neurobiology of potassium channels and epilepsy. Front Cell Neurosci. 2013; 7:134. [PubMed: 24062639]

de los Angeles Tejada M, Jensen LJ, Klaerke DA. PIP(2) modulation of Slick and Slack K(+) channels. Biochem Biophys Res Commun. 2012; 424:208–213. [PubMed: 22728883]

Du W, Bautista JF, Yang H, Diez-Sampedro A, You SA, Wang L, Kotagal P, Luders HO, Shi J, Cui J, et al. Calcium-sensitive potassium channelopathy in human epilepsy and paroxysmal movement disorder. Nat Genet. 2005; 37:733–738. [PubMed: 15937479]

Egan TM, Dagan D, Kupper J, Levitan IB. Na(+)-activated K+ channels are widely distributed in rat CNS and in Xenopus oocytes. Brain Res. 1992; 584:319–321. [PubMed: 1515948]

Fekete A, Franklin L, Ikemoto T, Rozsa B, Lendvai B, Sylvester Vizi E, Zelles T. Mechanism of the persistent sodium current activator veratridine-evoked Ca elevation: implication for epilepsy. J Neurochem. 2009; 111:745–756. [PubMed: 19719824]

Fisher RS, van Emde Boas W, Blume W, Elger C, Genton P, Lee P, Engel J Jr. Epileptic seizures and epilepsy: definitions proposed by the International League Against Epilepsy (ILAE) and the International Bureau for Epilepsy (IBE). Epilepsia. 2005; 46:470–472. [PubMed: 15816939]

Gao SB, Wu Y, Lu CX, Guo ZH, Li CH, Ding JP. Slack and Slick KNa channels are required for the depolarizing afterpotential of acutely isolated, medium diameter rat dorsal root ganglion neurons. Acta Pharmacol Sin. 2008; 29:899–905. [PubMed: 18664322]

Hage TA, Salkoff L. Sodium-activated potassium channels are functionally coupled to persistent sodium currents. J Neurosci. 2012; 32:2714–2721. [PubMed: 22357855]

Heron SE, Smith KR, Bahlo M, Nobili L, Kahana E, Licchetta L, Oliver KL, Mazarib A, Afawi Z, Korczyn A, et al. Missense mutations in the sodium-gated potassium channel gene KCNT1 cause severe autosomal dominant nocturnal frontal lobe epilepsy. Nat Genet. 2012; 44:1188–1190. [PubMed: 23086396]

Huang F, Wang X, Ostertag EM, Nuwal T, Huang B, Jan YN, Basbaum AI, Jan LY. TMEM16C facilitates Na(+)-activated K+ currents in rat sensory neurons and regulates pain processing. Nat Neurosci. 2013; 16:1284–1290. [PubMed: 23872594]

Ishii A, Shioda M, Okumura A, Kidokoro H, Sakauchi M, Shimada S, Shimizu T, Osawa M, Hirose S, Yamamoto T. A recurrent KCNT1 mutation in two sporadic cases with malignant migrating partial seizures in infancy. Gene. 2013; 531:467–471. [PubMed: 24029078]

Jiang Y, Lee A, Chen J, Cadene M, Chait BT, MacKinnon R. Crystal structure and mechanism of a calcium-gated potassium channel. Nature. 2002a; 417:515–522. [PubMed: 12037559]

Jiang Y, Lee A, Chen J, Cadene M, Chait BT, MacKinnon R. The open pore conformation of potassium channels. Nature. 2002b; 417:523–526. [PubMed: 12037560]

Joiner WJ, Tang MD, Wang LY, Dworetzky SI, Boissard CG, Gan L, Gribkoff VK, Kaczmarek LK. Formation of intermediate-conductance calcium-activated potassium channels by interaction of Slack and Slo subunits. Nat Neurosci. 1998; 1:462–469. [PubMed: 10196543]

Joshi D, Fung SJ, Rothwell A, Weickert CS. Higher gamma-aminobutyric acid neuron density in the white matter of orbital frontal cortex in schizophrenia. Biol Psychiatry. 2012; 72:725–733. [PubMed: 22841514]

Kameyama M, Kakei M, Sato R, Shibasaki T, Matsuda H, Irisawa H. Intracellular Na+ activates a K+ channel in mammalian cardiac cells. Nature. 1984; 309:354–356. [PubMed: 6328309]

Kim GE, Kaczmarek LK. Emerging role of the KCNT1 Slack channel in intellectual disability. Front Cell Neurosci. 2014; 8:209. [PubMed: 25120433]

Kim GE, Kronengold J, Barcia G, Quraishi IH, Martin HC, Blair E, Taylor JC, Dulac O, Colleaux L, Nabbout R, Kaczmarek LK. Human Slack Potassium Channel Mutations Increase Positive Cooperativity between Individual Channels. Cell Rep. 2014; 9:1661–1672. [PubMed: 25482562]

Kleinhans C, Kafitz KW, Rose CR. Multi-photon intracellular sodium imaging combined with UV-mediated focal uncaging of glutamate in CA1 pyramidal neurons. J Vis Exp. 2014:e52038. [PubMed: 25350367]

Lossin C, Rhodes TH, Desai RR, Vanoye CG, Wang D, Carniciu S, Devinsky O, George AL Jr. Epilepsy-associated dysfunction in the voltage-gated neuronal sodium channel SCN1A. J Neurosci. 2003; 23:11289–11295. [PubMed: 14672992]

Lu B, Su Y, Das S, Liu J, Xia J, Ren D. The neuronal channel NALCN contributes resting sodium permeability and is required for normal respiratory rhythm. Cell. 2007; 129:371–383. [PubMed: 17448995]

Mittmann T, Linton SM, Schwindt P, Crill W. Evidence for persistent Na+ current in apical dendrites of rat neocortical neurons from imaging of Na+-sensitive dye. J Neurophysiol. 1997; 78:1188–1192. [PubMed: 9307150]

Muller M, Somjen GG. Na(+) and K(+) concentrations, extra- and intracellular voltages, and the effect of TTX in hypoxic rat hippocampal slices. J Neurophysiol. 2000; 83:735–745. [PubMed: 10669489]

Niu X, Qian X, Magleby KL. Linker-gating ring complex as passive spring and Ca(2+)-dependent machine for a voltage- and Ca(2+)-activated potassium channel. Neuron. 2004; 42:745–756. [PubMed: 15182715]

Rose CR, Karus C. Two sides of the same coin: sodium homeostasis and signaling in astrocytes under physiological and pathophysiological conditions. Glia. 2013; 61:1191–1205. [PubMed: 23553639]

Salkoff L, Butler A, Ferreira G, Santi C, Wei A. High-conductance potassium channels of the SLO family. Nat Rev Neurosci. 2006; 7:921–931. [PubMed: 17115074]

Smart SL, Lopantsev V, Zhang CL, Robbins CA, Wang H, Chiu SY, Schwartzkroin PA, Messing A, Tempel BL. Deletion of the K(V)1.1 potassium channel causes epilepsy in mice. Neuron. 1998; 20:809–819. [PubMed: 9581771]

Soumier A, Sibille E. Opposing effects of acute versus chronic blockade of frontal cortex somatostatin-positive inhibitory neurons on behavioral emotionality in mice. Neuropsychopharmacology. 2014; 39:2252–2262. [PubMed: 24690741]

Tamsett TJ, Picchione KE, Bhattacharjee A. NAD+ activates KNa channels in dorsal root ganglion neurons. J Neurosci. 2009; 29:5127–5134. [PubMed: 19386908]

Tang QY, Zhang Z, Meng XY, Cui M, Logothetis DE. Structural determinants of phosphatidylinositol 4,5-bisphosphate (PIP2) regulation of BK channel activity through the RCK1 Ca2+ coordination site. J Biol Chem. 2014; 289:18860–18872. [PubMed: 24778177]

Tang QY, Zhang Z, Xia J, Ren D, Logothetis DE. Phosphatidylinositol 4,5-bisphosphate activates Slo3 currents and its hydrolysis underlies the epidermal growth factor-induced current inhibition. J Biol Chem. 2010; 285:19259–19266. [PubMed: 20392696]

Vanderver A, Simons C, Schmidt JL, Pearl PL, Bloom M, Lavenstein B, Miller D, Grimmond SM, Taft RJ. Identification of a novel de novo p.Phe932Ile KCNT1 mutation in a patient with leukoencephalopathy and severe epilepsy. Pediatr Neurol. 2014; 50:112–114. [PubMed: 24120652]

Wang J, Li Y, Hui Z, Cao M, Shi R, Zhang W, Geng L, Zhou X. Functional analysis of potassium channels in Kv7.2 G271V mutant causing early onset familial epilepsy. Brain Res. 2015; 1616:112–122. [PubMed: 25960349]

Whorton MR, MacKinnon R. Crystal structure of the mammalian GIRK2 K+ channel and gating regulation by G proteins, PIP2, and sodium. Cell. 2011; 147:199–208. [PubMed: 21962516]

Wu Y, Yang Y, Ye S, Jiang Y. Structure of the gating ring from the human large-conductance Ca(2+)-gated K(+) channel. Nature. 2010; 466:393–397. [PubMed: 20574420]

Yang B, Desai R, Kaczmarek LK. Slack and Slick K(Na) channels regulate the accuracy of timing of auditory neurons. J Neurosci. 2007; 27:2617–2627. [PubMed: 17344399]

Yang J, Krishnamoorthy G, Saxena A, Zhang G, Shi J, Yang H, Delaloye K, Sept D, Cui J. An epilepsy/dyskinesia-associated mutation enhances BK channel activation by potentiating Ca2+ sensing. Neuron. 2010; 66:871–883. [PubMed: 20620873]

Yu FH, Mantegazza M, Westenbroek RE, Robbins CA, Kalume F, Burton KA, Spain WJ, McKnight GS, Scheuer T, Catterall WA. Reduced sodium current in GABAergic interneurons in a mouse model of severe myoclonic epilepsy in infancy. Nat Neurosci. 2006; 9:1142–1149. [PubMed: 16921370]

Yuan A, Santi CM, Wei A, Wang ZW, Pollak K, Nonet M, Kaczmarek L, Crowder CM, Salkoff L. The sodium-activated potassium channel is encoded by a member of the Slo gene family. Neuron. 2003; 37:765–773. [PubMed: 12628167]

Yuan P, Leonetti MD, Pico AR, Hsiung Y, MacKinnon R. Structure of the human BK channel Ca2+-activation apparatus at 3.0 A resolution. Science. 2010; 329:182–186. [PubMed: 20508092]

Zeng XH, Yang C, Xia XM, Liu M, Lingle CJ. SLO3 auxiliary subunit LRRC52 controls gating of sperm KSPER currents and is critical for normal fertility. Proc Natl Acad Sci U S A. 2015

Zhang Y, Brown MR, Hyland C, Chen Y, Kronengold J, Fleming MR, Kohn AB, Moroz LL, Kaczmarek LK. Regulation of neuronal excitability by interaction of fragile X mental retardation protein with slack potassium channels. J Neurosci. 2012; 32:15318–15327. [PubMed: 23115170]

Zhang Z, Rosenhouse-Dantsker A, Tang QY, Noskov S, Logothetis DE. The RCK2 domain uses a coordination site present in Kir channels to confer sodium sensitivity to Slo2.2 channels. J Neurosci. 2010; 30:7554–7562. [PubMed: 20519529]

Zhang Z, Tang QY, Alaimo JT, Davies AG, Bettinger JC, Logothetis DE. SLO-2 isoforms with unique Ca(2+) - and voltage-dependence characteristics confer sensitivity to hypoxia in C. elegans. Channels (Austin). 2013; 7:194–205. [PubMed: 23590941]

Highlights

- Epilepsy-related Slack channel mutants increase channel maximal open probability
- Seven mutants related to epilepsy enhance sodium sensitivity of Slack channel
- The Y775H mutant directly facilitates sodium binding of Slack channel
- Two mutants exhibit their over-activity only in high intracellular sodium concentration

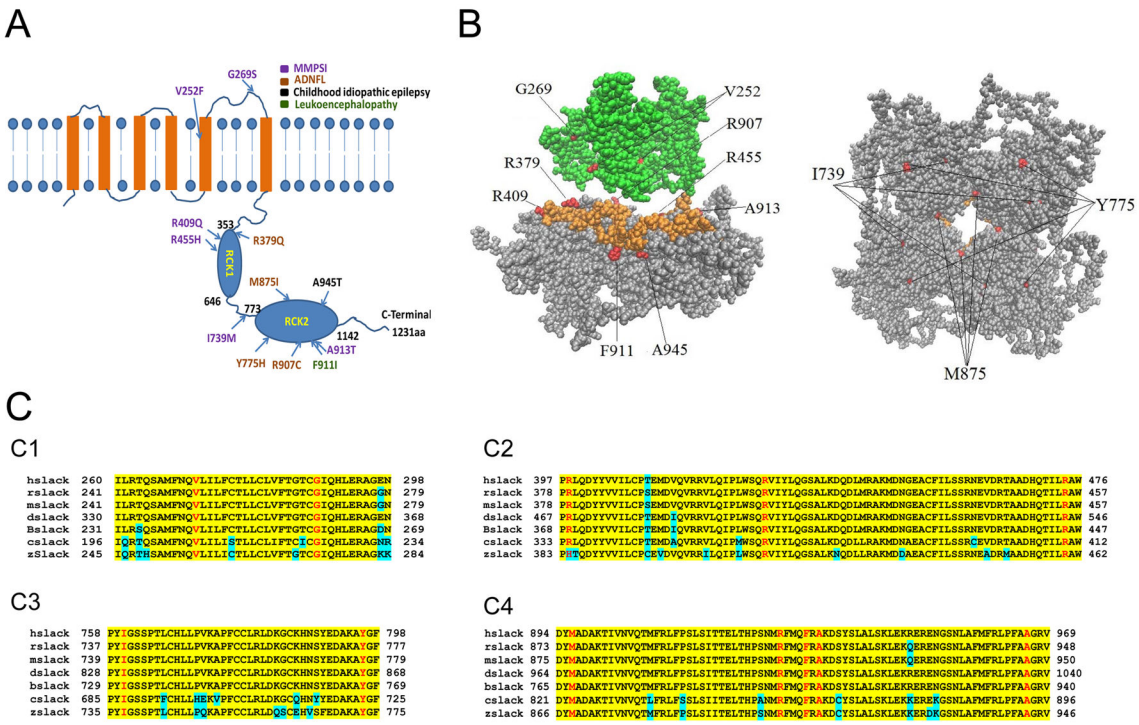

Figure 1. Spatial distribution and conservation of the epilepsy-related amino acid residues of the Slack channel

(A) Schematic representation of the Slack channel. The N- and C- termini are localized inside the cell. Four subunits together form the pore in the plasma membrane of the cell. The long C-terminus includes two RCK domains (RCK, regulators of conductance of K^+). The positions of epilepsy related mutants are indicated in red on the schematic. **(B)** The Slack channel homology model structure used a template that the Kv1.2/Kv2.1 pore domain (green) is superimposed on the Slo1 channel C terminus (grey but with AC region highlighted in orange, the N terminus of the RCK1 domain containing 76 amino acids, a region including the secondary structures βA-αC named as AC region) (Left, side view). The structure of gating ring of the Slack channel is shown without the pore domain (Right, bottom view). **(C)** Sequence alignment for the context region of epilepsy related Slack channel mutants. The amino acid residues related to epilepsy are shown in red. Conservative residues in the indicated species are shown (**C1**) V252, G269 (**C2**) R379, R409 and R455 (**C3**) I739 and Y775 (**C4**) M875, R907, F911, A913 and A945. Human Slack (hslack) Gene ID (GI): 57582, Rat Slack (rslack) GI: 60444, Mouse Slack GI: 227632, Dog Slack (dslack) GI: 491258, Bovine Slack GI: 529468, Chicken Slack (cslack) GI: 395248, Zebrafish Slack (zslack) GI: 100004419. Conserved amino residues are shown with yellow background. Non-conserved residues are shown with cyan background.

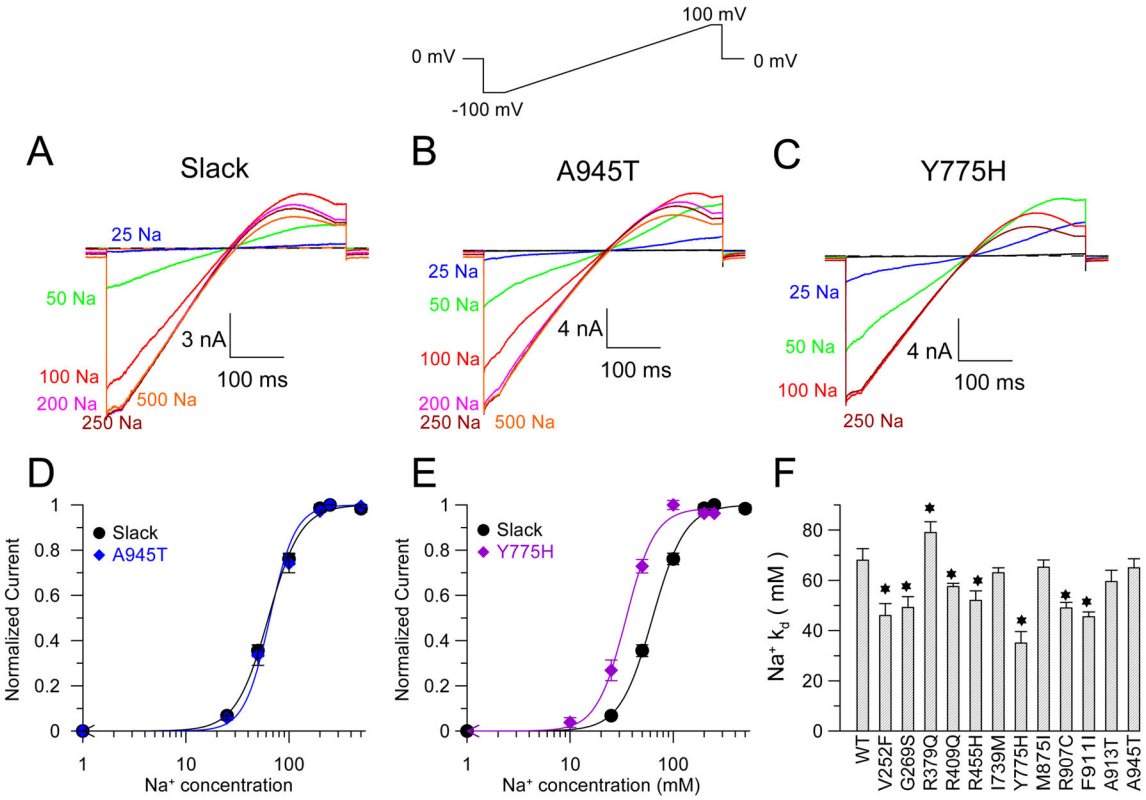

Figure 2. Seven epilepsy related mutants enhance sodium sensitivity of Slack channel

(A–C) Macroscopic typical current traces recorded from inside-out patches expressing WT **(A)**, A945T **(B)** and Y775H mutants **(C)** respectively. Currents were elicited in 0 – 500 mM $[Na^+]_i$ by a ramp protocol from −100 mV to +100 mV. **(D–E)** Sample Hill equation fits of the Na^+ dose-response for macroscopic current data of WT (K_d of 68±6 mM, Co-efficient number: n=2.9) vs A945T (k_d of 65± 3.6 mM, n=3.3). **(D)** (K_d of 65±3.6 mM, n=3.3) and **(E)** WT vs Y775H (K_d of 35 ± 3.4 mM, *n*=3) respectively. **(F)** Summary of Na^+ sensitivity of K_d values for Slack mutants related to epilepsy. WT (K_d of 68±4.6 mM, n=2.9), V252F (K_d of 46±4.7 mM, n=3), G269S (K_d of 49.2±4.3 mM, n=3.3), R379Q (K_d of 83±4.3 mM, n=3.5), R409Q (k_d of 57.5±1.3 mM, n=3.6), R455H (k_d of 52±3.8 mM, n=2.7), I739M (K_d of 63±2 mM, n=3), Y775H (k_d of 35±4.6 mM, n=3.1), M875I (k_d of 65.2±2.9 mM, n=3.2), R907C (K_d of 49±4.3 mM, n=3.1), F911A (K_d of 45.5±1.9 mM, n=3.0), A913T (k_d of 59.5±4.5 mM, n=2.9) and A945T (k_d of 65±3.6 mM, n=3.3).

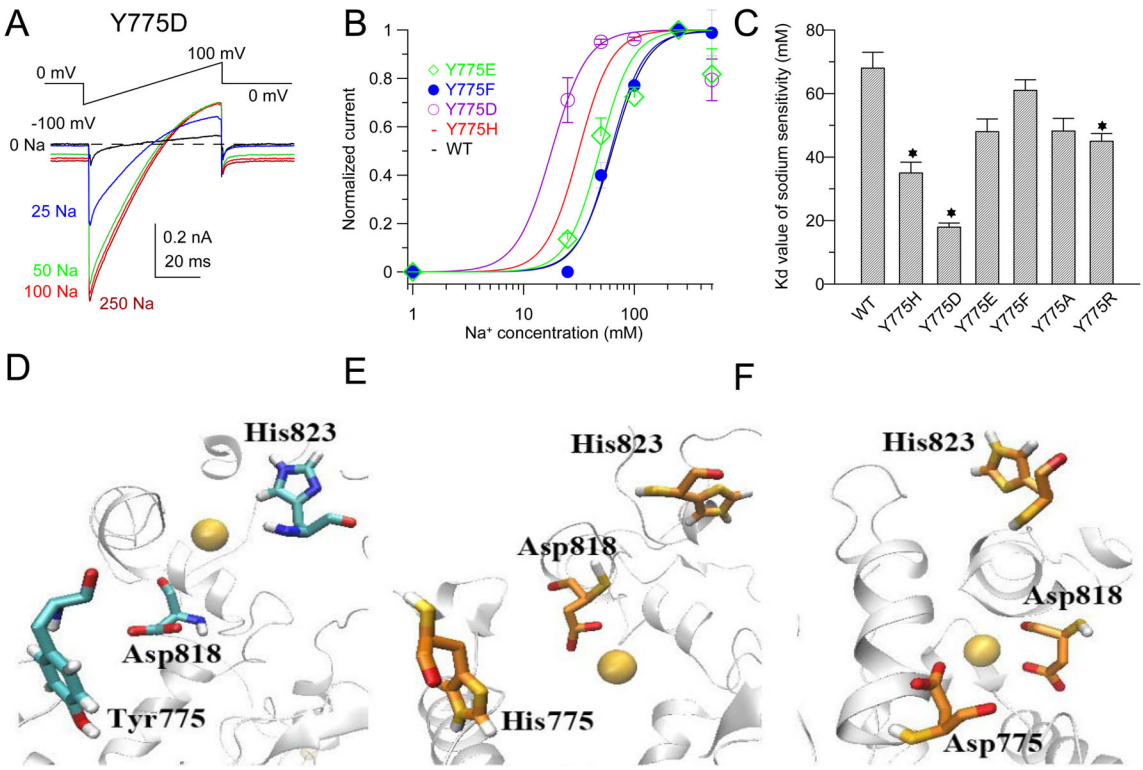

Figure 3. Y775H and Y775D mutants are directly involved in conferring sodium sensitivity to Slack channels

(A) Typical current traces recorded in the inside-out patch configuration for Y775D, the ramp protocol ran from −100 mV to +100 mV. **(B)** Hill equation fits of the Na^+ dose–response data of the wild-type Slack channel, Y775H, Y775F, Y775E and Y775D mutants. **(C)** Summary of K_d values for the wild-type Slack (K_d of 68±6 mM, n=2.9) and the Y775 mutants (Y775H K_d of 35 ± 3.4 mM, n =3.1; Y775D K_d of 17.9 ±1.3 mM, n=3.2; Y775E K_d of 48 ± 4 mM, n=3.1; Y775F K_d of 61 ± 3.3 mM, n=2.9; Y775A K_d of 48.2 ± 4 mM, n=3.0; Y775R K_d of 45 ± 2.4 mM, n=3.1) * indicates the mean values of groups are significantly different from the wild-type Slack channel. **(D)** Local structure of sodium binding site of wild type Slack channel homology model. The Y775 (phenol ring in blue and other bond in cyan), sodium ion (yellow sphere), D818 and H823 (nitrogen ring in blue and other bond in cyan) belongs to the sodium coordination site of the wild-type Slack channel. In the wild-type channel, the Y775 residue is not positioned parallel to H823 residue and is not involved in sodium binding. **(E)** The local sodium sensing site structure of the Y775H mutant structure on the homology model. The H775 (nitrogen ring with N atom in yellow and the other bond in orange), sodium ion (yellow sphere), D818 (bond in orange and the carboxylate of D818 in red) and H823 (Nitrogen ring with nitrogen atom in yellow and other bond in orange) form the sodium co-ordinate site of Y775H mutant. In the Y775H mutant, the sodium binds with D818 and is flanked by the H823 and H775 residues. **(F)** Local structure of the Slack channel Y775D mutant sodium binding site on the homology model.

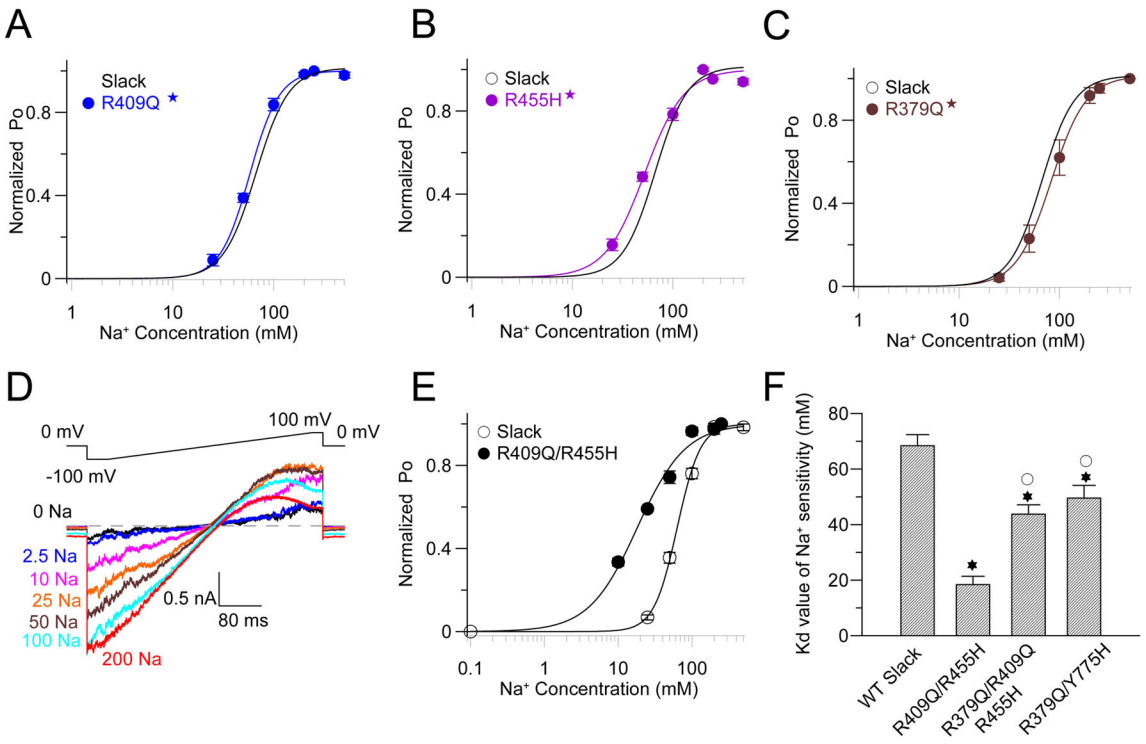

Figure 4. Epilepsy-related mutants localized on the RCK1 domain cause an independent conformational change to shift the sodium sensitivity of Slack channels

(A–C) Sample Hill equation fits of the Na^+ dose-response macroscopic current data of WT and R409Q (K_d of 57.5±1.3 mM, n=3.3), WT and R455H (K_d of 52 ± 3.8 mM, n=2.7), WT and R379Q (K_d of 83±5.3 mM, n=3) respectively. ★ indicates the mean values of groups are significantly different from the mean value of the wild-type Slack channel. **(D)** Typical macroscopic current traces recorded in the inside-out patch configuration for R409Q/R455H with $[Na^+]_i$ from 0–200 mM. **(E)** Na^+ dose–response data were fitted with the Hill equation for the wild-type Slack channel, R409Q/R455H mutant. **(F)** Summary of K_d values for the wild-type Slack (WT K_d of 68±6 mM, n=2.9, R409Q/R455H, K_d of 18.4 ± 3 mM, n=1.5, R409Q/R455H/R379Q, K_d of 43.8 ± 3.4 mM, n=3, R379Q/Y775H, K_d of 49.6 ± 4.5 mM, n=3.2) * indicates the mean values of groups are significantly different from the mean value of the wild-type Slack channel. ○ indicates the mean values of groups are significantly different from the mean value of R455H/R409Q groups and R379Q groups.

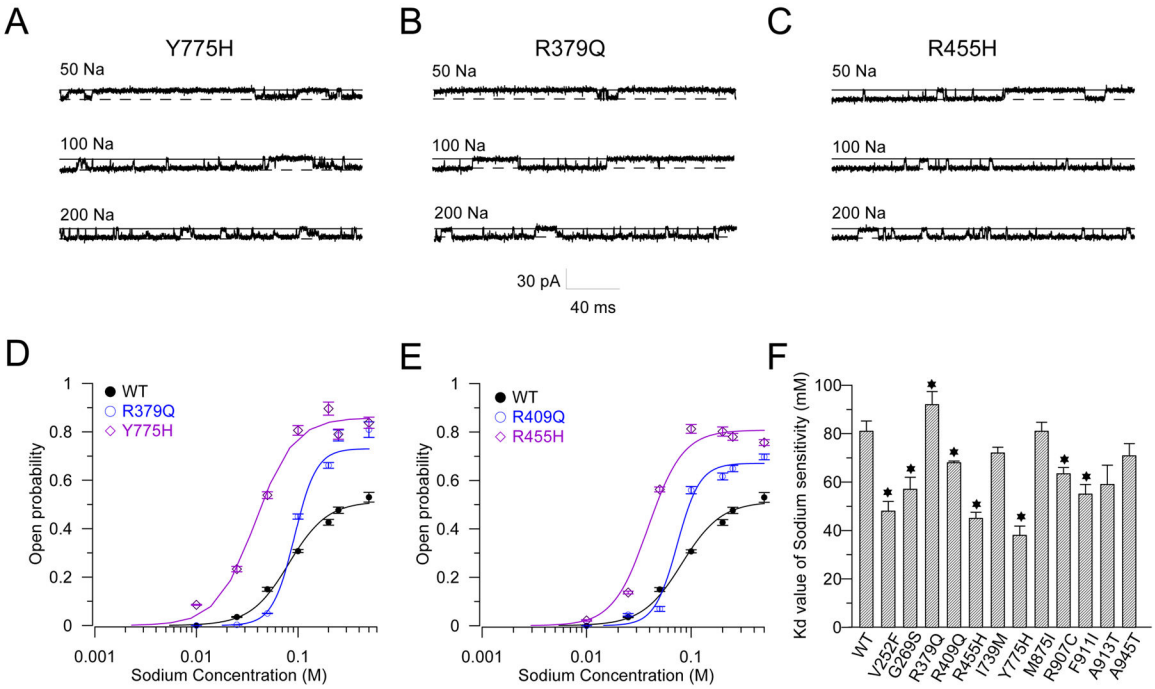

Figure 5. Single-channel recordings reveal that epilepsy related mutants not only alter the sodium sensitivity but also enhance the maximal P_o of the Slack channel

(A–C) Typical single channel traces with $[Na^+]_i$ from 50–200 mM of Y775H **(A)**, R379Q **(B)** and R455H **(C). (D–E)** Sodium dose-dependent single-channel open probabilities (P_o) of mutants are fitted by the Hill equation. The coefficient factors are indicated in the n value. (**D)** Slack WT: K_d = 81±3.7, n=3.3; P_{max} = 0.57±0.02; R379Q: K_d = 92±5.4 mM, n=4; P_{max} = 0.81±0.012, Y775H: K_d = 38 ± 3.8 mM, n = 2.3; P_{max} = 0.9±0.027. (**E**) R455H: K_d = 45±2.5 mM, n=4, R409Q: K_d = 68±0.7mM, n=4 **(F.)** Summary of K_d values obtained from single channel recording by fitting Po of the epilepsy-related Slack channels mutants with the Hill equation.

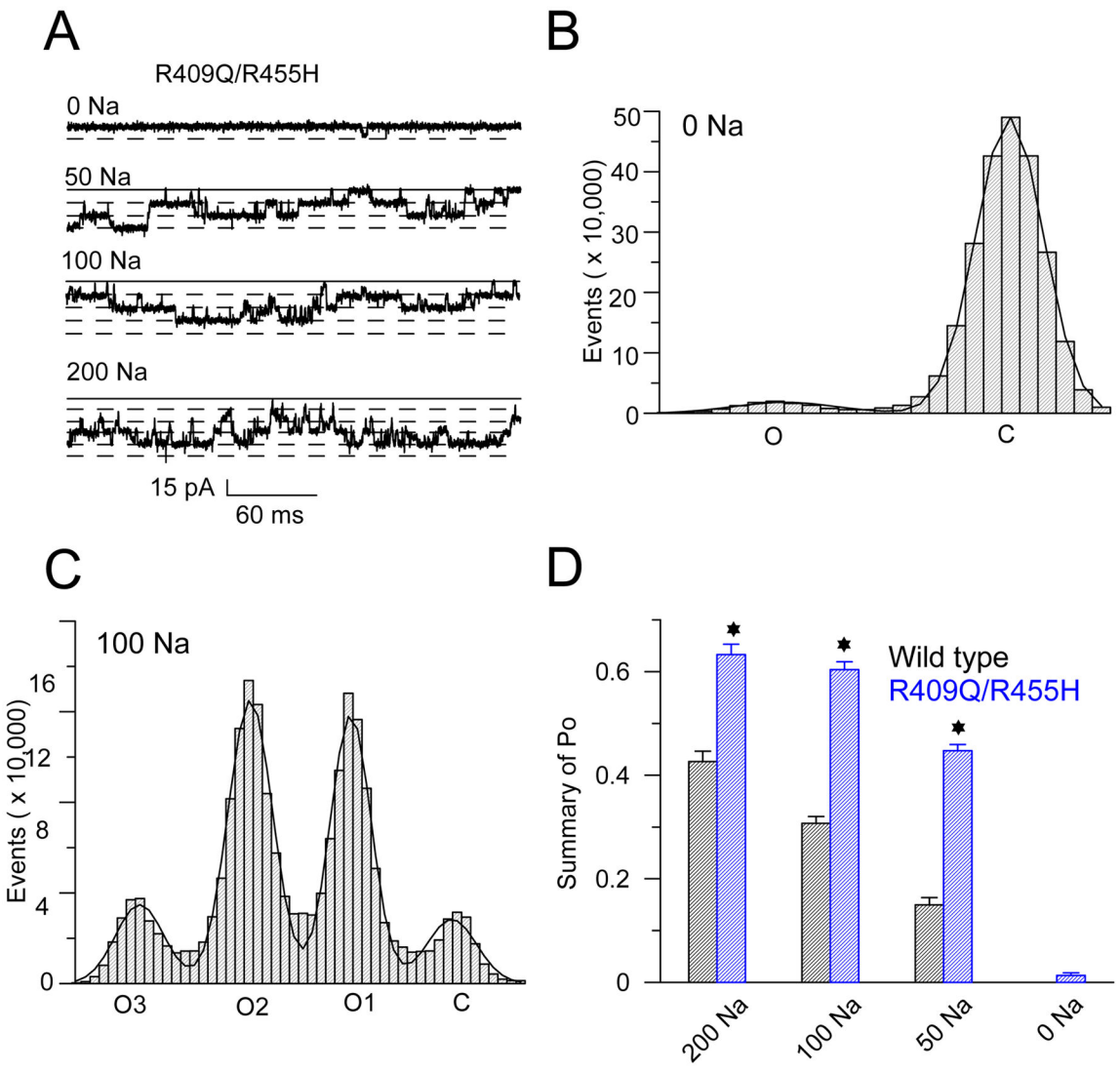

Figure 6. Double mutant R409Q/R455H not only enhances channel sodium sensitivity but also leads to channel opening in the absence of Na^+

(A) Typical single-channel recording current traces in the inside-out patch configuration for R409Q/R455H with 0–200 mM $[Na^+]_i$ **(B)** The total amplitude histogram of R409Q/R455H in single-channel recording events in 0 mM $[Na^+]_i$ were fitted by a Gaussian function. Each number in the *y*-axis is times 10,000 events. **(C)** R409Q/R455H double mutant amplitude histogram with 100 mM $[Na^+]_i$ were fitted with a Gaussian function. **(D)** Comparison of averaged P_o values of WT Slack channel (Black) with P_o values of R409Q/R455H mutant (Blue) in different concentrations of $[Na^+]_i$. P_o of wild type Slack channel is not measurable in 0 mM $[Na^+]_i$, $P_o = 0.15 \pm 0.01$ in 50 mM $[Na^+]_i$, $P_o = 0.31 \pm 0.03$ in 100 mM $[Na^+]_i$, $P_o = 0.43 \pm 0.02$ in 200 mM $[Na^+]_i$. R409Q/R455H (Blue) $P_o = 0.013 \pm 0.005$ in 0 mM $[Na^+]_i$, $P_o = 0.45 \pm 0.012$ in 50 mM $[Na^+]_i$, $P_o = 0.74 \pm 0.012$ in 100 mM $[Na^+]_i$, $P_o = 0.75 \pm 0.02$ in 200 mM $[Na^+]_i$).

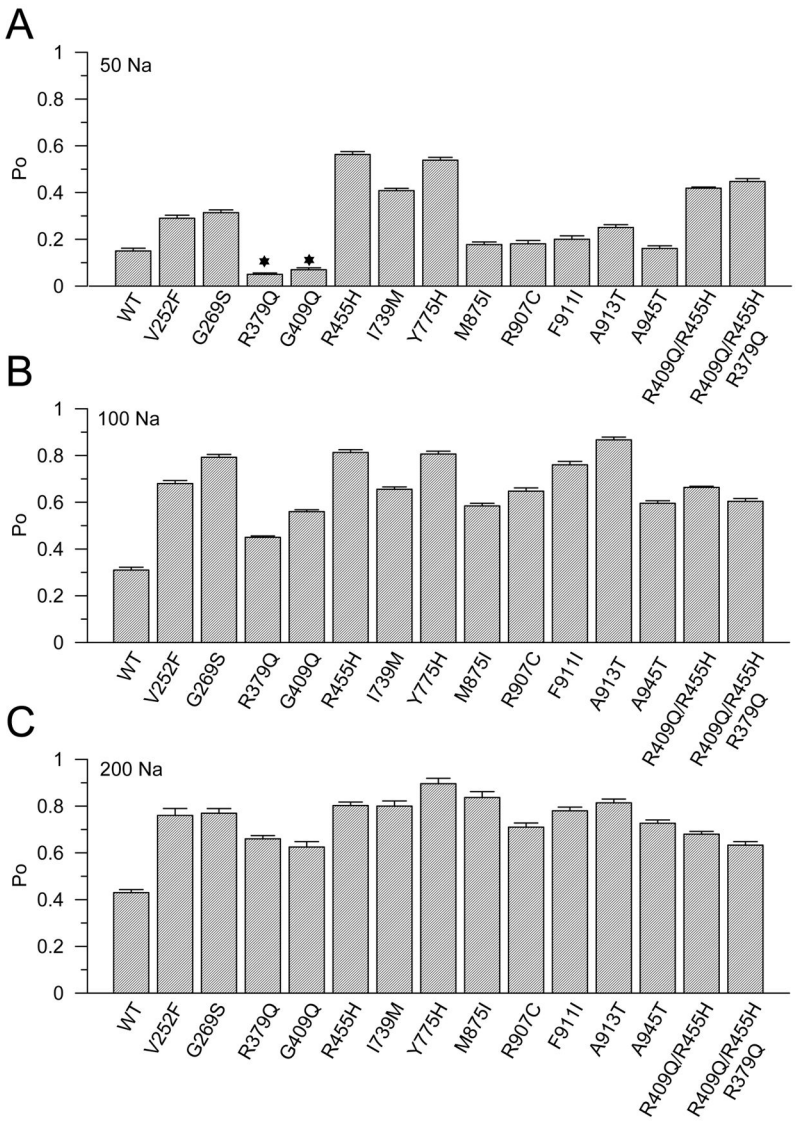

Figure 7. Some Slack channel mutants show uniform increases in P_o at high concentrations of $[Na^+]_i$

P_o of all mutants are summarized in increasing $[Na^+]_i$ A to C, respectively. **(A)** The P_o of all mutants in 50 mM $[Na^+]_i$ are shown. **(B)** The P_o of all mutants in 100 mM $[Na^+]_i$ are shown. (**C**) The P_o of all mutants in 200 mM $[Na^+]_i$ are shown. The percentage numbers of P_o were summarized in Table S1 and Table S2.